Temperature dependence of the size distribution function of InAs quantum dots on GaAs(001)

F. Arciprete, M. Fanfoni, F. Patella, A. Della Pia, and A. Balzarotti
Dipartimento di Fisica, Università di Roma "Tor Vergata," Via della Ricerca Scientifica 1, I-00133 Roma, Italy

E. Placidi
CNR-CNISM, Via della Ricerca Scientifica 1, I-00133 Roma, Italy

(Received 12 August 2009; revised manuscript received 22 December 2009; published 7 April 2010)

We present a detailed atomic-force-microscopy study of the effect of annealing on InAs/GaAs(001) quantum dots grown by molecular-beam epitaxy. Samples were grown at a low growth rate at 500 °C with an InAs coverage slightly greater than critical thickness and subsequently annealed at several temperatures. We find that immediately quenched samples exhibit a bimodal size distribution with a high density of small dots (<50 nm^3) while annealing at temperatures greater than 420 °C leads to a unimodal size distribution. This result indicates a coarsening process governing the evolution of the island size distribution function which is limited by the attachment-detachment of the adatoms at the island boundary. At higher temperatures one cannot ascribe a single rate-determining step for coarsening because of the increased role of adatom diffusion. However, for long annealing times at 500 °C the island size distribution is strongly affected by In desorption.

DOI: 10.1103/PhysRevB.81.165306 PACS number(s): 68.55.A−, 68.55.J−, 81.15.Hi

In recent years, III-V self-assembled quantum dots (QDs) have been studied extensively for their potential as lasers emitting at 1.3 μm at room temperature with low-threshold current density,[1] and single photon emitters for nanophotonics and quantum computing.[2] The emission wavelength is deeply related to the size and shape of QDs; consequently understanding the evolution of these quantities is of primary importance, also as regards the possibility of tuning the energy spectrum of QDs.

It is well known that post-growth heating is responsible for several processes which influence the size distribution and the shape of islands, i.e., coarsening, where the larger islands grow at the expense of the smaller ones which shrink and disappear, and intermixing with the substrate atoms. The relative importance of these processes depends on annealing conditions and initial configuration after deposition. Emission wavelength tuning and sharpening after annealing have been proved for InAs QDs grown on both unpatterned and patterned GaAs(001) substrates;[3] annealing effects on faceting of QDs have recently been demonstrated for the InAs/GaAs(001) system.[4] The study of the evolution of the size distribution of islands during deposition and post-growth annealing is therefore fundamental for applications and for an insight into the processes controlling size and uniformity.

In this paper we present an atomic-force-microscopy (AFM) study of the effect of annealing on InAs/GaAs(001) quantum dots grown by molecular-beam epitaxy. By measuring the size distribution function of QDs as a function of the annealing time and temperature we identify the different regimes of coarsening and the mechanisms which govern the evolution of the size distribution. Thus, the results which we present in this work provide important insights regarding the stability of QDs and the physical conditions for narrowing the island size distribution.

Prior to InAs deposition, a GaAs buffer layer of approximate thickness 500 nm was grown at 590 °C on the (001)-oriented substrate, in As_4 overflow, at a rate of 0.8 μm/h. Once the buffer layer was deposited, the surface was flattened by 30 min post-growth annealing at 660 °C under an As_4 beam equivalent pressure (BEP): 4.0×10^{-5} torr.[5] For all the samples studied, we deposited 1.63 ML of InAs at a rate of 0.032 ML/s at 500 °C, when a clear $c(4\times4)$ reconstruction of the GaAs surface was observed. Immediately after the InAs growth, the samples were annealed under As_4 flux (BEP$=6.0\times10^{-6}$ Torr) at 420, 460, and 500 °C. For purposes of comparison, samples without post-growth annealing and immediately quenched after the InAs deposition were also grown. The reflection high-energy electron-diffraction pattern was monitored by a charge-coupled device camera during growth and annealing. AFM VEECO multiprobe characterization was performed *ex situ* in the tapping mode by using ultrasharp nonconductive Si tips with a nominal radius of about 2 nm.

Figure 1 shows five representative AFM topographies of 1.63 ML of InAs deposited on the GaAs(001) surface: (a) after prompt quenching, (b) after annealing at 420 °C for 30 min, (c) at 460 °C for 30 min, (d) at 500 °C for 5 min, and finally (e) at 500 °C for 30 min. Panel (a) shows the presence of small and large QDs, the former having a height and lateral dimensions ranging from 0.6 to 1.5 nm and from 10 to 20 nm, respectively, the latter having a height larger than 2 nm and lateral dimensions ranging from 20 to 30 nm. Faceting and aspect ratio (AR) of the large islands are compatible with a pyramid shape with {137} facets—apart from the sample with no annealing where {136} facets are found as well[4]—while small islands are, in effect, unfaceted.[6,7]

Recent experimental papers[8,9] have suggested that, for annealing temperatures ranging from 440 to 475 °C, coarsening of QDs in the InAs/GaAs(001) system is an Ostwald ripening (OR), where the process is limited by atom attachment/detachment at the dot edges. Our results summarized in Table I corroborate the hypothesis of coarsening: the mean volume of QDs increases and their density decreases as a function of temperature and of annealing time. Nonetheless, we will show below that other mechanisms are acting besides coarsening.

The OR theory describes a process in which islands are immobile but adatoms move to and from islands. The driving

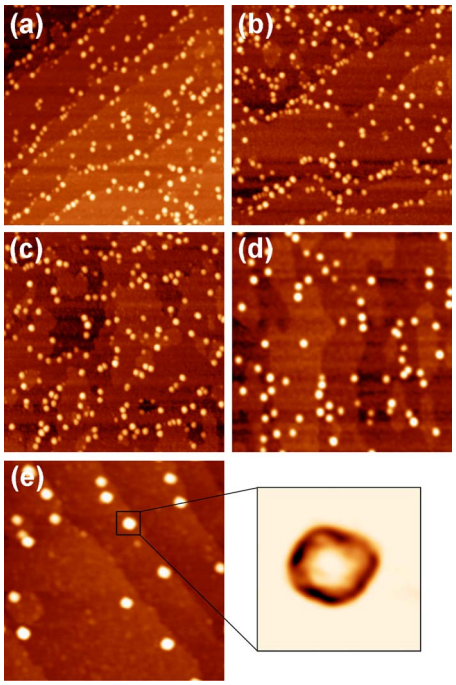

FIG. 1. (Color online) AFM topographies (600×600 nm^2) of 1.63 ML of InAs deposited on the GaAs(001) surface: (a) after prompt quenching, (b) after annealing at 420 °C for 30 min, (c) at 460 °C for 30 min, (d) at 500 °C for 5 min, and (e) at 500 °C for 30 min. The inset shows a slope image of the selected area (80×80 nm^2) of panel (e) and the color scale corresponds to the local surface slope with respect to the substrate plane.

force for the growth originates from the adatoms' concentration gradients around the islands, where the adatoms detachment from the islands obeys the Gibbs-Thomson equation. Thus, it is possible to define a critical radius R_c such that the detachment probability of adatoms from islands with radius $R<R_c$ is much larger than from islands with radius $R>R_c$.[10] Moreover, the OR theory predicts that the island size distribution function, $f(R,t)$, is asymptoptically time independent and can be expressed in a scale invariant form $f(x)$, where $x=R/R_c$. The kinetics of OR is usually discussed in two limiting cases depending on two rate-determining processes: diffusion-limited (DL) and attachment-detachment-limited (ADL). The former is the OR process described above. The latter, in which the processes at the islands' edge limit the kinetics, also called reaction limited, is characterized by a chemical-potential constant among the islands and discontinuous at the island edges. The invariant distribution function is obtained from the solution of the continuity equation. For the two-dimensional DL case[11] it yields

TABLE I. Statistical analysis of the volume distribution of QDs: mean volume ($\langle V\rangle$), standard deviation of the normalized distribution ($\sigma_V/\langle V\rangle$), number density ($\rho$), and total volume contained in QDs (V_T).

Annealing	$\langle V\rangle$ (nm^3)	$\sigma_V/\langle V\rangle$	ρ (cm^{-2})	V_T (ML)
None	148	0.79	5.8×10^{10}	0.29
30 min-420 °C	143	0.69	6.0×10^{10}	0.29
30 min-460 °C	269	0.56	5.4×10^{10}	0.48
5 min-500 °C	491	0.35	1.8×10^{10}	0.30
30 min-500 °C	861	0.67	6.7×10^{9}	0.19
30 min-500 °C-no platelets	1421	0.34	3.9×10^{9}	0.19

$$f_{\mathrm{DL}}(x)=\begin{cases} C4x^3\left(\frac{4}{3}-x\right)^{-19/6}\left(x^2+\frac{8}{3}x+\frac{16}{3}\right)^{-23/12}\exp\left(\frac{-2}{4-3x}\right)\exp\left[-\frac{1}{6\sqrt{2}}\tan^{-1}\left(\frac{3x+4}{4\sqrt{2}}\right)\right] & x<\frac{4}{3} \\ 0 & x>\frac{4}{3}, \end{cases} \tag{1}$$

where C is a normalization constant. If the rate-limiting step is the ADL from the islands, the distribution function is[11,12]

$$f_{\mathrm{ADL}}(x)=\begin{cases} C'\dfrac{x}{(2-x)^5}\exp\left(\dfrac{-6}{2-x}\right) & x<2 \\ 0 & x>2. \end{cases} \tag{2}$$

Also in this case C' is a normalization constant.

In order to describe our results within the theoretical framework of OR, a set of histograms has been created as a function of $V^{1/3}$ [Figs. 2(a)–2(e)]. To produce the size distributions, several AFM images (300×300 nm^2) representative of the surface have been analyzed for each sample. The total number of dots ranged from 300 to 500 depending on the QDs density. In order to compare the theoretical distribution functions [Eqs. (1) and (2)] to the experimental histograms, the former have been standardized, i.e.,: $\int_0^\infty f(x)dx=1$, and $\int_0^\infty xf(x)dx=1$, the latter have been plotted against the scaled variable $x=V^{1/3}/\langle V^{1/3}\rangle$ and normalized to unity. The resulted histograms are shown in Figs. 2(f)–2(j) and, from now on, they will be addressed as standardized distributions (SD).

The bimodal distribution of dots shown in Figs. 2(a) and 2(f) (no annealing) has been reported several times.[13–16] We should stress that a similar scenario has been observed during the growth of Ge on Si(001).[7,17–19] For the case of Ge/Si(001) system, Ross *et al.*[18] have provided a theoretical explanation in which the occurrence of a shape transition is

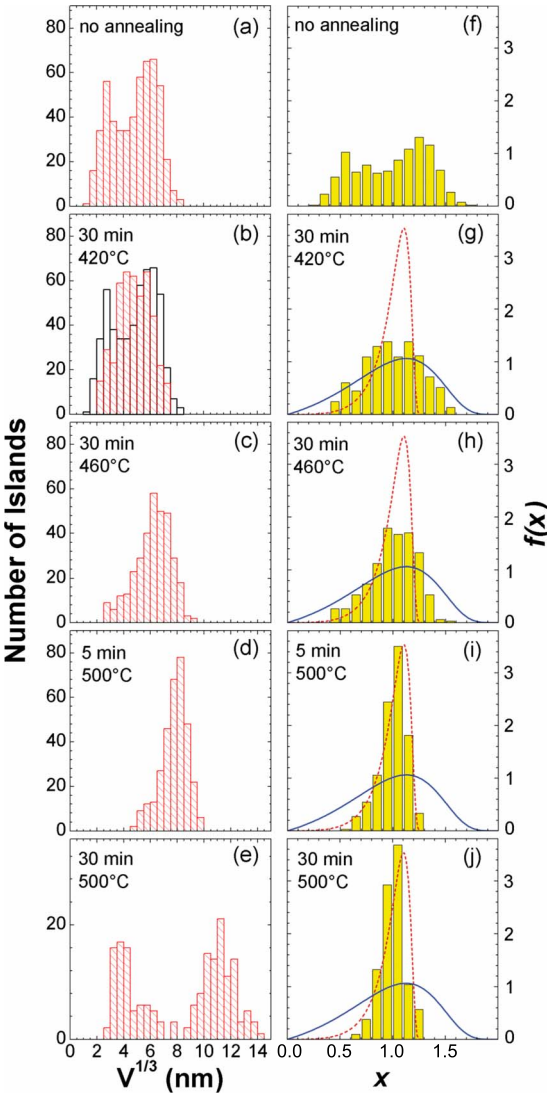

FIG. 2. (Color online) [(a)–(e)]: $V^{1/3}$ histograms as a function of annealing temperature and time. Panel (a) is superimposed to (b) for comparison. [(f)–(j)]: corresponding experimental standardized distribution of (a)–(e) plotted as a function of the scaling variable $x = V^{1/3}/\langle V^{1/3}\rangle$. The theoretical scaling functions $f_{\mathrm{ADL}}(x)$ (continuous line) and $f_{\mathrm{DL}}(x)$ (dashed line) are reported for comparison. In panel 2(e) the distribution at low volume refers to flat platelets (see text).

accompanied by a sudden reduction in the chemical potential and gives rise to anomalous ripening and the development of a bimodal distribution of sizes. Our findings reinforce the analogy between the two model systems.

The size distributions after annealing, shown in Figs. 2(b)–2(d) and 2(g)–2(i), are unimodal. In particular, Figs. 2(b)–2(d) display a mean value which increases with increasing temperature, a trend suggesting that coarsening must have occurred. In Fig. 2(e) we observe the unexpected reappearance of a bimodal distribution. This effect can be clarified after a careful analysis of the AFM topographies such as the one reported in Fig. 3. It is evident that small islands turn out to be flat platelets ~1 ML high. A likely interpretation is that either they are remnants of the coarsening process, where QDs have shrunk in favor of the larger ones [a similar

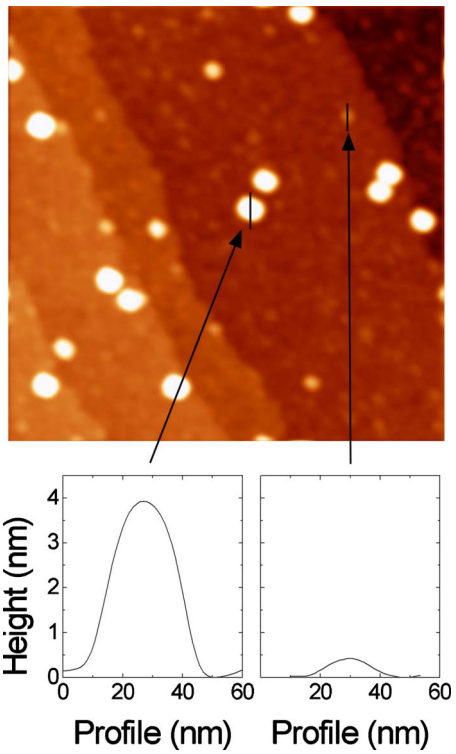

FIG. 3. (Color online) 600×600 nm^2 AFM topography after 30 min of annealing at 500 °C. Lower panels show profiles of large quantum dots (left panel) and flat platelets (right panel).

effect has been observed on the Ge/Si(001) system[20]] or simply have evaporated[21] (see discussion below). For this reason in Fig. 2(j) only the distribution at large $V^{1/3}$ has been taken into account and the platelets have been excluded from the statistical analysis.

Although the change from a bimodal [Figs. 2(a) and 2(f)] to unimodal [Figs. 2(b)–2(e) and 2(g)–2(j)] QDs size distribution demonstrates that a coarsening process is underway, it is not the only process even at the lowest annealing temperature of 420 °C. In Fig. 2(b) we have superimposed, for a direct comparison, the distribution of Fig. 2(a) (black empty histogram) to the distribution obtained after annealing at 420 °C. It is evident that, not only do the smaller QDs dissolve in favor of the larger ones (as expected for a standard coarsening process) but, because of the elastic barrier due to strain at the island edges, also the largest QDs lose atoms making the distribution more symmetrical in a kind of self-sizing process.[22] This latter statement is corroborated by the fact that, after annealing, the transition from {136} facets to {137} facets, is accompanied by a reduction in the respective volume of the QDs.[4] In Fig. 2(g) the sample annealed at $T = 420$ °C exhibits a broad and unimodal SD which does not differ significantly from the theoretical curve described by Eq. (2) (continuous line). The small change in the SD observed is ascribed to the self-sizing process cited above, which makes the SD quite symmetric. In fact, its skewness is almost zero [$Skw(420) = -0.08$] and much greater than that of the theoretical scaling function [$Skw(f_{\mathrm{ADL}}) = -0.43$].

After annealing at 460 °C the size distribution function [Fig. 2(c)] is modified: The volume mean value increases,

the distribution shows a clear reduction in the standard deviation, becomes more asymmetric, and the QDs density decreases of about 10% (Table I). This is evidence of a coarsening process occurring on the surface. On the other hand, in Fig. 2(h) the SD is plotted along with the theoretical functions $f_{\mathrm{ADL}}(x)$ (continuous line) and $f_{\mathrm{DL}}(x)$ (dashed line). Neither $f_{\mathrm{ADL}}(x)$ nor $f_{\mathrm{DL}}(x)$ describe the SD. A discussion about the applicability of Eqs. (1) and (2) as descriptions of the Ostwald ripening is therefore necessary. Both theories are correct for an infinitely dilute distribution of islands and do not take into account competitive effects on the growth process. Several attempts to include these effects have been made leading to a broadening of the distribution and to a shift of its maximum to higher values of x.[23,24] A large island, for example, grows faster when surrounded by smaller islands than when surrounded by islands of similar size. Actually, these correlations act to spread the distribution function, contrary to our experimental observations [see the evolution from Figs. 2(h)–2(j)]. More important for the system under study, standard OR models are based on the assumption that the total volume of the islands is constant, i.e., they hold only for conservative system, while it is well known[25–28] that in the InAs/GaAs(001) system an important mass transfer to the QDs from both the wetting layer (WL) and the substrate occurs for temperature $\gtrsim$450 °C, contributing to the total volume contained in QDs. Moreover, also at 460 °C the self-sizing process cited above contributes to filling in the distribution around the mean value. Therefore, in view of these facts, it is not surprising to find poor agreement between theory and experiment in Fig. 2(h).

At 500 °C the annealing time becomes crucial. Within the first five minutes, with respect to the sample with no annealing, we observe an increase in the mean volume of QDs, a reduction in their number density but, particularly important here, the total volume contained in the QDs remains constant (Table I). These facts indicate that coarsening is faster than WL and substrate erosion.[29] As far as the moments of the SD are concerned, the comparison with the 460 °C data evidences a reduction in both the standard deviation (Table I), and the skewness [from $Skw(460)=-0.44$ to $Skw(500,5)=-0.66$]. All these observations justify the comparison between experimental and theoretical SDs: The inspection of Fig. 2(i) suggests that the DL theory explains better the experimental SD than the ADL theory.[30] A change from ADL to DL kinetics implies higher-energy barriers for monomer diffusion among the islands. As a matter of fact, the calculated diffusion coefficient of In is much lower on GaAs surface than on strained InAs/GaAs surface.[31,32] So, the interdiffusion process, which increases the surface Ga concentration at 500 °C,[33] reducing the strain, is responsible for such increase in the barrier energies. Unfortunately, reliable theoretical calculations which corroborate our discussion are at present not available.

Annealing the sample for 30 min does not change the standard deviation further but determines a clear reduction in the total volume contained in QDs (Table I) and reincreases the skewness [$Skw(500,30)=-0.27$] of the SD which becomes more symmetrical [see Fig. 2(j)]. By considering the reduction in the total volume V_{T} contained in QDs the OR theory is not applicable and the SD is probably the result of the competition between coarsening, WL/substrate erosion and desorption. In addition, a sharp reduction in the AR of QDs is observed, as illustrated in Fig. 4. Similar results have been obtained on SiGe/Si(001) where a drop of the aspect ratio, driven by Si-Ge interdiffusion, was ascribed to a QDs shape transition from dome to pyramid.[34] Although our AFM images prevent us fixing the exact shape of QDs, the slope image shows that the large dots in Fig. 1(e) are flat on their top (see the inset in Fig. 1). In Ref. 4 it was shown that, besides a considerable increase in QDs' mean volume, after 30 min of annealing at 500 °C, the AR decreases and the QDs shape changes from pyramid to a truncated pyramid or flat dome (see also Fig. 3 of Ref. 4). These results do not conflict with experimental findings in the literature,[6,7,34] where an AR increase follows the transition from pyramid to dome. In fact, because of the long period of annealing at 500 °C, significant In desorption and In-Ga intermixing between the islands and the substrate might have been occurred so increasing the Ga concentration in QDs and flattening the QDs shape, as predicted by theory.[35]

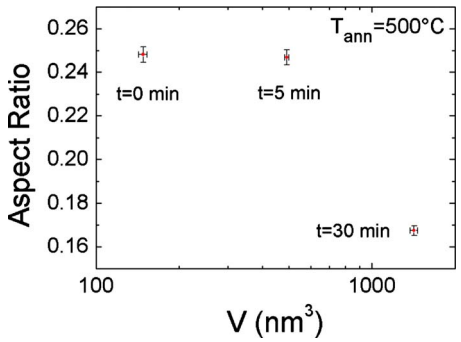

FIG. 4. (Color online) Average QD aspect ratio vs mean volume at 500 °C as a function of the annealing time.

The QDs evolution at 500 °C provides a rough estimate of the time scale of the extra processes besides coarsening given the variation of the island density ρ, the total volume contained in QDs V_{T}, and the QDs aspect ratio, relative to the unannealed sample. ρ is reduced by ~69% and ~93% after 5 and 30 min annealing, respectively, while V_{T} and AR remain, in fact, constant after 5 min of annealing but undergo a huge reduction (~35% for V_{T}) after 30 min of annealing (see Table I). All these facts imply that the effects of desorption on QDs at $T=500$ °C are remarkable only for long annealing times[36] as further evidenced by the reported dissolution of QDs occurring at high temperatures.[8,21] In addition, the larger evaporation rate of the small dots makes the SD more symmetric as substantiated by the analysis of the skewness [from $Skw(500,5)=-0.66$ to $Skw(500,30)=-0.27$].

In conclusion, we have studied by means of atomic-force microscopy the after-growth evolution of the size distribution function of InAs/GaAs(001) quantum dots grown by molecular-beam epitaxy. The results clearly indicate that the evolution of the size distributions can be understood within the framework of the Ostwald ripening theory provided the total island volume is conserved. We have found that after 30 min of annealing at $T=420$ °C experimental data are fitted by the theory in the limit of attachment-detachment rate de-

termining step. By increasing the temperature of annealing at $T=460$ °C the WL/substrate erosion becomes progressively more important and concurrent with the coarsening process: after 30 min of annealing time the system is no longer conservative and the OR theory is not applicable. Nonetheless, for short annealing time (5 min) at $T=500$ °C, the total volume of islands is conserved and the experiment is well described by the OR theory when the rate-determining process is diffusion. This implies higher-energy barriers for monomer diffusion with respect to the annealing at $T=420$ °C. Finally, for annealing longer than 5 min the islands' size distribution is the result of the competition between coarsening, intermixing and In desorption.

We acknowledge the support of the MIUR PRIN-2007 of Italy under Contract No. 2007S4FAA4.

[1] D. L. Huffaker, G. Park, Z. Zou, O. B. Shchekin, and D. G. Deppe, Appl. Phys. Lett. **73**, 2564 (1998).
[2] Z. Yuan, B. E. Kardynal, R. M. Stevenson, A. J. Shields, C. J. Lobo, K. Cooper, N. S. Beattie, D. A. Ritchie, and M. Pepper, Science **295**, 102 (2002).
[3] S. Kiravittaya, A. Rastelli, and O. G. Schmidt, Rep. Prog. Phys. **72**, 046502 (2009).
[4] E. Placidi, A. Della Pia, and F. Arciprete, Appl. Phys. Lett. **94**, 021901 (2009).
[5] Z. Ding, D. W. Bullock, P. M. Thibado, V. P. LaBella, and K. Mullen, Phys. Rev. Lett. **90**, 216109 (2003).
[6] K. Jacobi, Prog. Surf. Sci. **71**, 185 (2003).
[7] G. Costantini, A. Rastelli, C. Manzano, R. Songmuang, O. G. Schmidt, K. Kern, and H. von Kanel, Appl. Phys. Lett. **85**, 5673 (2004).
[8] D. M. Schaadt, D. Z. Hu, and K. H. Ploog, J. Vac. Sci. Technol. B **24**, 2069 (2006).
[9] R. Kremzow, M. Pristovsek, and M. Kneissl, J. Cryst. Growth **310**, 4751 (2008).
[10] For a review see: P. W. Voorhees, J. Stat. Phys. **38**, 231 (1985); M. Zinke-Allmang, L. C. Feldman, and M. H. Grabow, Surf. Sci. Rep. **16**, 377 (1992); A. Baldan, J. Mater. Sci. **37**, 2171 (2002).
[11] B. K. Chakraverty, J. Phys. Chem. Solids **28**, 2401 (1967).
[12] C. Wagner, Z. Elektrochem. **65**, 581 (1961).
[13] T. R. Ramachandran, R. Heitz, P. Chen, and A. Madhukar, Appl. Phys. Lett. **70**, 640 (1997).
[14] F. Arciprete, E. Placidi, V. Sessi, M. Fanfoni, F. Patella, and A. Balzarotti, Appl. Phys. Lett. **89**, 041904 (2006).
[15] E. Placidi, F. Arciprete, M. Fanfoni, F. Patella, E. Orsini, and A. Balzarotti, J. Phys.: Condens. Matter **19**, 225006 (2007).
[16] A. Balzarotti, Nanotechnology **19**, 505701 (2008).
[17] G. Medeiros-Ribeiro, A. M. Bratkovsky, T. I. Kamins, D. A. A. Ohlberg, and R. S. Williams, Science **279**, 353 (1998).
[18] F. M. Ross, J. Tersoff, and R. M. Tromp, Phys. Rev. Lett. **80**, 984 (1998).
[19] T. I. Kamins, G. Medeiros-Ribeiro, D. A. A. Ohlberg, and R. Stanley Williams, J. Appl. Phys. **85**, 1159 (1999).
[20] A. Rastelli, M. Stoffel, J. Tersoff, G. S. Kar, and O. G. Schmidt, Phys. Rev. Lett. **95**, 026103 (2005).
[21] Ch. Heyn, Phys. Rev. B **66**, 075307 (2002).
[22] T. I. Kamins and R. Stanley Williams, Surf. Sci. **405**, L580 (1998).
[23] A. J. Ardell, Phys. Rev. B **41**, 2554 (1990).
[24] A. Chakrabarti, R. Toral, and J. D. Gunton, Phys. Rev. E **47**, 3025 (1993).
[25] P. B. Joyce, T. J. Krzyzewski, G. R. Bell, B. A. Joyce, and T. S. Jones, Phys. Rev. B **58**, R15981 (1998).
[26] F. Patella, A. Sgarlata, F. Arciprete, S. Nufris, P. D. Skutznik, E. Placidi, M. Fanfoni, N. Motta, and A. Balzarotti, J. Phys.: Condens. Matter **16**, S1503 (2004).
[27] E. Placidi, F. Arciprete, V. Sessi, M. Fanfoni, F. Patella, and A. Balzarotti, Appl. Phys. Lett. **86**, 241913 (2005).
[28] T. Honma, S. Tsukamoto, and Y. Arakawa, Jpn. J. Appl. Phys. **45**, L777 (2006).
[29] T. J. Krzyzewski and T. S. Jones, J. Appl. Phys. **96**, 668 (2004) come to the same conclusion after annealing the sample at $T=485$ °C.
[30] On the other hand, Shaadt *et al.* (Ref. 8), who maintain that at 475 °C the kinetics is ADL, do not reach any definitive conclusion for $T=500$ °C.
[31] M. Rosini, M. C. Righi, P. Kratzer, and R. Magri, Phys. Rev. B **79**, 075302 (2009).
[32] E. Penev, S. Stojković, P. Kratzer, and M. Scheffler, Phys. Rev. B **69**, 115335 (2004).
[33] Ch. Heyn and W. Hansen, J. Cryst. Growth **251**, 140 (2003).
[34] M. Stoffel, A. Rastelli, J. Stangl, T. Merdzhanova, G. Bauer, and O. G. Schmidt, Phys. Rev. B **75**, 113307 (2007).
[35] B. J. Spencer and J. Tersoff, Phys. Rev. Lett. **79**, 4858 (1997).
[36] F. Patella, F. Arciprete, M. Fanfoni, A. Balzarotti, and E. Placidi, Appl. Phys. Lett. **88**, 161903 (2006).